Hindawi Publishing Corporation
Journal of Nanomaterials
Volume 2014, Article ID 857614, 7 pages
http://dx.doi.org/10.1155/2014/857614

Research Article

Effects of Hydrogen on the Optical and Electrical Characteristics of the Sputter-Deposited Al_2O_3-Doped ZnO Thin Films

Fang-Hsing Wang,[1] Cheng-Fu Yang,[2] Jian-Chiun Liou,[3] and In-Ching Chen[1]

[1] *Department of Electrical Engineering and Graduate Institute of Optoelectronic Engineering, National Chung Hsing University, Taichung 402, Taiwan*
[2] *Department of Chemical and Materials Engineering, National University of Kaohsiung, Kaohsiung 811, Taiwan*
[3] *Electronics and Optoelectronics Research Laboratories, Industrial Technology Research Institute, Hsinchu 310, Taiwan*

Correspondence should be addressed to Cheng-Fu Yang; cfyang@nuk.edu.tw

Received 22 October 2013; Accepted 13 January 2014; Published 9 March 2014

Academic Editor: Hong Seok Lee

In this study, AZO thin films were deposited on glass by using a 98 mol% ZnO + 1 mol% Al_2O_3 (AZO, Zn : Al = 98 : 2) ceramic target and a r.f. magnetron sputtering system. At first, the effects of different H_2 flow rates ($H_2/(H_2 + Ar)$ = 0%~9.09%, abbreviated as H_2-deposited AZO thin films, deposition temperature was 200°C) added during the deposition process on the physical and electrical properties of AZO thin films were investigated. The optical transmittance at 400 nm~700 nm is more than 80% for all AZO thin films regardless of H_2 flow rate and the transparency ratio decreased as the H_2 flow rate increased. The Burstein-Moss shift effect was used to prove that the defects of AZO thin films decreased with increasing H_2 flow rate. Also, the 2% H_2-deposited AZO thin films were also treated by the H_2 plasma at room temperature for 60 min (plasma-treated AZO thin films). The value variations in the optical band gap (E_g) values of the H_2-deposited and plasma-treated AZO thin films were evaluated from the plots of $(\alpha h\nu)^2 = c(h\nu - E_g)$, and the E_g values increased with increasing H_2 flow rate. The E_g values also increased as the H_2-plasma process was used to treat on the H_2-deposited Al_2O_3-doped ZnO (AZO) thin films.

1. Introduction

Zinc oxide (ZnO), which is an n-type oxide semiconductor with a wurtzite crystal structure, is a novel II–VI compound semiconductor with various electrical, optical, acoustic, and chemical properties because of its wide direct band gap of 3.40 eV at room temperature. ZnO-based thin films are also good candidates to substitute for indium tin oxide (ITO) and tin oxide (SnO_2) thin films in amorphous silicon (α-Si) solar cells because they are stable in the hydrogen plasma, whereas ITO and SnO_2 produce a metallic layer in the reducing plasma [1]. Additionally, in the case of $CuInSe_2$- and $CuInGaSe_2$-based heterojunction solar cells [2], ZnO coatings used as window layers have been found to enhance the current more than the standard CdS (or ZnS) coatings, due to ZnO's higher band gap. Nonstoichiometric, undoped ZnO thin films have usually shown low resistivity due to the oxygen vacancies and zinc interstitials [3]. Hydrogen almost never occurs as an electrically neutral impurity inside a semiconductor or insulator. Invariably, it either (i) gives up its electron, becoming positively charged and acting as a donor in p-type semiconductors, or (ii) acquires an additional electron, becoming negatively charged and acting as an acceptor in n-type semiconductors. Therefore, hydrogen has the properties of an amphoteric impurity, when it is used as the atmosphere during the deposition process or used as the plasma after the films deposition, it will change the conductivity of formed thin films [4].

However, hydrogen is exclusively in a positively charged state when calculations show, and only the positively charged state occurs in ZnO. Thus, hydrogen can only act as a dopant, and other charge states cannot be stabilized in ZnO-based semiconductors [5]. In the past, several methods had been studied to improve the properties of ZnO-based thin films. Oh et al. reported the effects of different substrate temperatures on the crystallization behavior and optical properties of

ZnO and AZO thin films [6]. Strzhemechny et al. reported on how the crystallization behavior and optical properties of AZO thin films were affected by the addition of hydrogen during the deposition process [7]. In this study, a 98 mol% ZnO + 1 mol% Al_2O_3 (AZO, Zn : Al = 98 : 2) compound was used as the target, and radio frequency (RF) magnetron sputtering was developed as a viable fabrication technique to deposit AZO thin films. In the past, the deposition temperature of AZO thin films was changed from room temperature to 300°C. We had studied the effect of deposition temperature on the physical and electrical properties of AZO thin films [8]. In this study, hydrogen (H_2) was used during the deposition process and as plasma gas of AZO thin films. We would further investigate the effects of H_2 on the physical and electrical properties of AZO thin films. At first, different H_2 flow rates ($H_2/(H_2 + Ar)$ = 0~9.09%) were added in Argon during the deposition process (abbreviated as the H_2-deposited AZO thin films). Next, the deposited AZO thin films were treated by the H_2 plasma (abbreviated as plasma-treated AZO thin films). The effects of H_2 flow rates and H_2 plasma on the properties of AZO thin films were compared by observing the crystallization, resistivity and optical transmission spectrum. Optical transmission parameters were also used to investigate the effects of H_2 flow rate and H_2 plasma on the optical band gap of AZO thin films.

2. Experimental Details

AZO powder ($ZnO : Al_2O_3$ = 98 : 2, mole ratio) was calcined at 1100°C and sintered at 1350°C to prepare the ceramic target. AZO thin films were deposited on 25 mm × 25 mm × 2 mm Corning 1737 glass substrates by using the r.f. magnetron sputtering system. The argon or argon-hydrogen were introduced into the chamber and the pressure was controlled at 5×10^{-2} Torr, under the 30 sccm with the different $H_2/(H_2 + Ar)$ flow rates (0%~9.09%, abbreviated as H_2-deposited AZO thin films). The r.f. power was 100 W and the deposition temperature (200°C) was controlled by a thermocouple gauge. All AZO thin films had a thickness of about 120 nm by controlling the deposition time. After deposition, the plasma enhanced chemical vapor deposition (PECVD) hydrogen (H_2) was treated on the as-deposited AZO thin films (plasma-treated AZO thin films) for 60 min. The working pressure was maintained at 1 Torr under the 300 sccm H_2 flow rate and the used power was 10 W. The chemical bonding states of oxygen, aluminum, and zinc in AZO thin films were investigated using an X-ray photoelectron spectroscopy (XPS) (ULVAC-PHI, PHI 5000 Versaprobe). The electrical resistivity was measured using a four-point probe, the optical transmittance spectrum was recorded using a Hitachi U-3300 UV/Vis spectrophotometer in the 300–800 nm wavelength range.

3. Results and Discussion

Surface images of the as-deposited and plasma-treated AZO thin films are shown in Figure 1. It is evident that H_2 flowing rate and plasma-treated process have large effects on the films' surface morphologies. At first, the grain sizes increase with increasing H_2 flowing rate and reach the maximum at 2%, then the grain sizes decrease as the H_2 flowing rate is further increased. However, as Figures 1(a)–1(d) show, AZO thin films deposited at different H_2 flowing rate samples yielded rough and rugged surfaces. Also, as the H_2 flowing rate is increased, the roughness is apparently lessened because larger particle coalescence is observable causing major grain growth. When the H_2 plasma is used to treat on the deposited AZO thin films, the roughness is apparently improved, as Figures 1(e)–1(h) show. From the surface morphologies shown in Figure 1, the H_2 flowing rate and plasma-treated process will have the large effects on the physical and electrical properties of AZO thin films.

The XRD patterns of the Ar-deposited, 2% H_2-deposited, and plasma-treated 2% H_2-deposited AZO thin films were investigated, and the results are shown in Figure 2. The (002) peaks of the Ar-deposited, 2% H_2-deposited, and plasma-treated 2% H_2-deposited AZO thin films are situated at around 2θ = 34.61°, 34.37°, and 34.27°, respectively. These results imply that the parameter of lattice constant c decreases as H^+ ions are used in the fabrication process. The H^+ ions doping into AZO thin films and having smaller ion radius can cause these results. The full width at half maximum (FWHM) values for the (002) peak are 0.33, 0.24, and 0.28 for the Ar-deposited, 2% H_2-deposited, and plasma-treated 2% H_2-deposited AZO thin films, respectively. These results suggest that the H_2-deposited and plasma-treated 2% H_2-deposited AZO thin films have the better crystalline structure.

Figure 3 shows the transmittance spectra of the H_2-deposited AZO thin films plotted against the different H_2 flow rate and wavelengths in the region of 300–800 nm. As Figure 3 shows, the optical transmittance at 400 nm~700 nm is more than 80% for all AZO thin films regardless of H_2 flow rate. The transparency ratio of the H_2-deposited AZO thin films decreased as the H_2 flow rate increased. This result is due to the crystallization and the density of AZO thin films decrease. In the transmission spectra of the H_2-deposited AZO thin films, the optical band edges are shifted to a shorter wavelength and a greater sharpness is noticeable in the curves of absorption edges as compared with those of Ar-deposited AZO thin films. Those results mean that as the H_2 flow rate increases, the absorption edge of AZO thin films is blue-shifted. In the past, determination of the optical band gap (E_g) was often necessary to develop the electronic band structure of a thin-film material. However, using extrapolation methods, the E_g values of thin films can be determined from the absorption edge for direct interband transition, which can be calculated using the relation in (3) as follows:

$$(\alpha h\nu)^2 = c\left(h\nu - E_g\right), \tag{1}$$

where α is the optical absorption coefficient, c is the constant for direct transition, h is Planck's constant, and ν is the frequency of the incident photon [9]. The linear dependence of $(\alpha h\nu)^2$ on $h\nu$ indicates that AZO thin films are direct transition type semiconductors. In accordance with (3), the calculated optical band gap of the H_2-deposited AZO thin

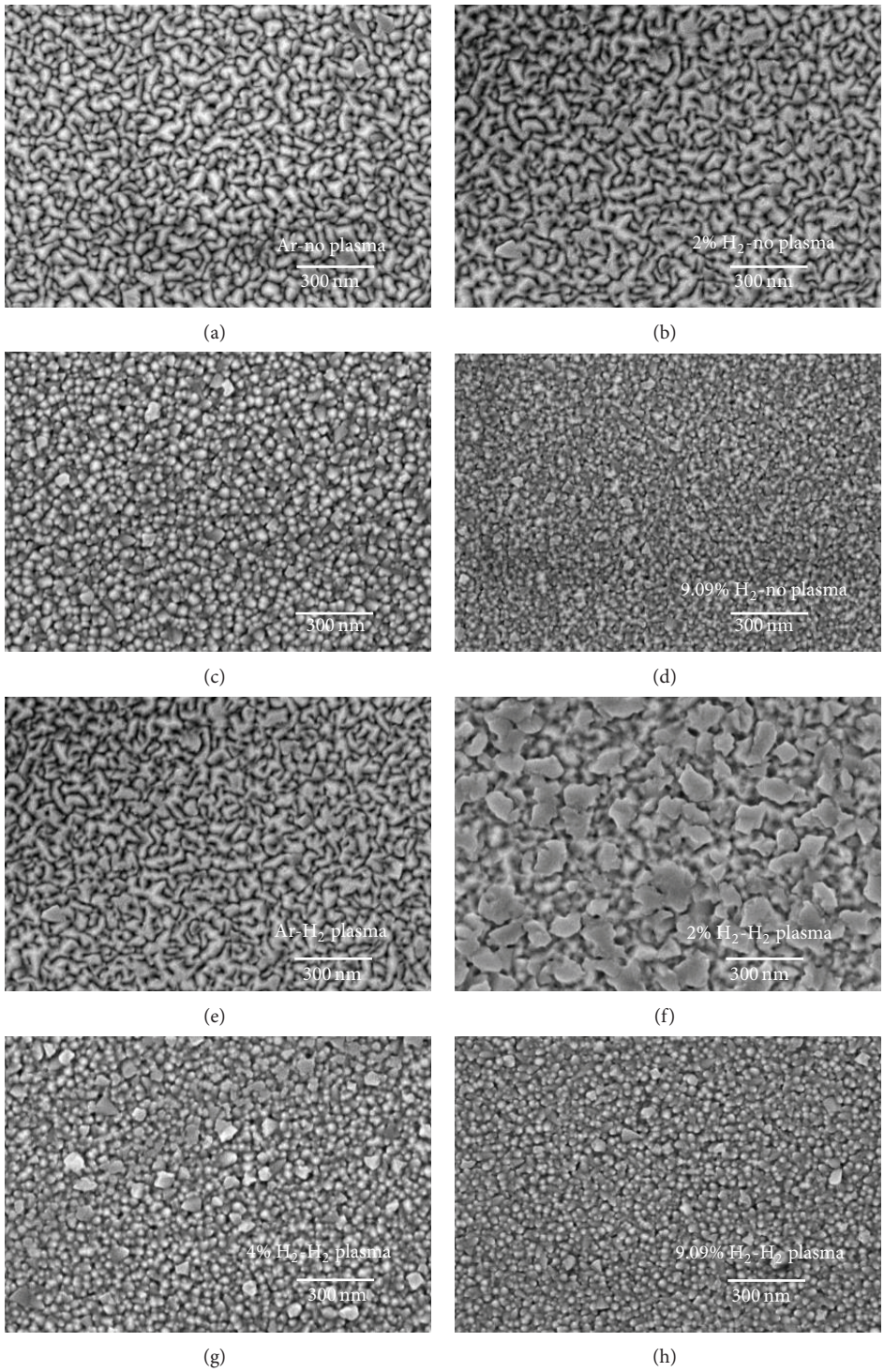

Figure 1: SEM observations of AZO thin films as a function of $H_2/(H_2 + Ar)$ flowing rate, for the as-deposited samples (a) 0%, (b) 2%, (c) 4%, and (d) 9.09%, and for the as-deposited and plasma-treated samples (e) 0%, (f) 2%, (g) 4%, and (h) 9.09%.

films increased from 3.74 to 3.82 eV as H_2 flowing rate increased.

Figure 4 shows the energy band gap of the plasma-treated AZO thin films plotted against wavelengths in the region of 300–800 nm. In the transmission spectra of the plasma-treated 2% H_2-deposited AZO thin films, the optical band edge is also shifted to a shorter wavelength and a greater sharpness is also noticeable in the curves of the absorption edge as compared with those of the H_2-deposited AZO thin films shown in Figure 3. The plasma-treated 2% H_2-deposited AZO thin films are also the optimal H_2 content, because they have the minimum resistivity (Figure 6). The calculated

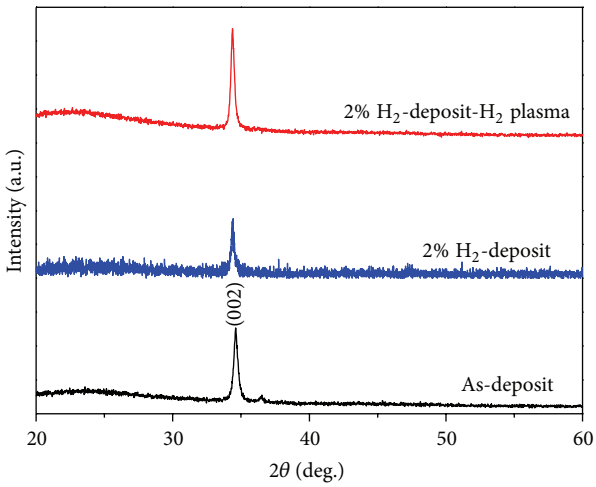

FIGURE 2: XRD patterns of the Ar-deposited, 2% H_2-deposited, and plasma-treated 2% H_2-deposited AZO thin films.

optical band gap of the plasma-treated 2% H_2-deposited AZO thin films also increased from 3.77 to 3.83 eV as the H_2 flow rate increased. The optical transmittance at 400 nm~700 nm is more than 83% for all thin films regardless of H_2 flow rate.

This blue-shift can be explained by the Burstein-Moss shift, a shift of Fermi level into the conduction band, which enhances the optical band gap by the energy, as follows [10, 11]:

$$\Delta E_g^{\mathrm{BM}} = \frac{\hbar^2 k_F^2}{2}\left(\frac{1}{m_e} + \frac{1}{m_h}\right) = \frac{\hbar^2 k_F^2}{2m_{vc}^*}, \tag{2}$$

where the k_F stands for the Fermi wave vector, m_e is the effective mass of electrons in the conduction band, and m_h is the effective mass of holes in the valence band, which can be simplified as m_{vc}^*; the Burstein-Moss shift ΔE_g^{BM} can be rewritten by inducing k_F for the carrier concentration n_e as follows:

$$\Delta E_g^{\mathrm{BM}} = \frac{h^2}{8m_{vc}^*}\left(\frac{3n_e}{\pi}\right)^{2/3}, \tag{3}$$

where h is the Planck's constant. Equation (3) shows the important relationship between the Burstein-Moss shift and the carrier concentration n_e. The shift of the absorption edge to the shorter wavelength region is due to the increase in carrier concentration. When the wavelength is equal to 300 nm, the visible light absorbed by the thin films is due to a quantum phenomenon called band edge absorption. Burstein indicated that an increase of the Fermi level in the conduction band of a degenerated semiconductor leads to the energy band widening effect [10, 11]. For that, the movement of the absorption edge to the shorter wavelength region is the Burstein-Moss shift.

From (3), we know that the shift of the optical band edge is caused by the increase in carrier concentration. This is because the Fermi level inside the conduction band moves upward with increasing donor concentration due to the filling of conduction band by the increase of carrier concentration [12]. Those results suggest that the addition of H_2 in the Ar as the deposition atmosphere can increase the carrier concentration. The absorption edge shifts monotonically to the shorter wavelength region as the hydrogen flow rate increases. This is because the Fermi level inside the conduction band moves upward with increasing donor concentration due to the filling of conduction band by the increase of carrier concentration [12].

The E_g value of ZnO thin films is about 3.40 eV and, in general, the measured E_g values of AZO thin films are consistent with and should be larger than that of ZnO thin films, because the E_g value of Al_2O_3 is about 6.55 eV. As the 98 mol% ZnO + 1 mol% Al_2O_3 composition is used as the target to deposit AZO thin films, the E_g value of AZO thin films can be calculated as

$$E_g = 0.98 \times 3.40 + 0.02 \times 6.55 = 3.46. \tag{4}$$

The blue-shift (ΔE_g) values are calculated from the difference between 3.46 eV and the E_g values obtained in Figures 3 and 4. Figure 5 shows the ΔE_g values of the H_2-deposited and the plasma-treated 2% H_2-deposited AZO thin films as a function of carrier concentration. It is found that the ΔE_g values are approximately proportional to n_e, and AZO thin films deposited at higher H_2 content exhibit a stronger blue-shift phenomenon. These results show that when the H_2 is used in the deposition processes, the E_g values become larger. This means that the blue-shift in the plasma-treated process has the same phenomenon, because H_2 will cause the growth of AZO thin films. Those results also suggest that the H_2 atoms also provide the electronic influences of AZO thin films, resulting in the increase of carrier concentration, however causing a blue-shift phenomenon.

To estimate the relation between ΔE_g and n_e quantitatively, set $m^* = 0.28\, m_0$, where m_0 is the free electron mass, and substitute measured values of ΔE_g and n_e into (3). The calculated corresponding exponent is about 0.64 for all the AZO thin films regardless of H_2 addition and H_2 plasma treatment. Oh et al. [13] also reported that the exponent is 0.655 from their Burstein-Moss shift measurement of AZO thin films, and other researches [14, 15] show that the exponents are in the range from 1/3 to 2/3. They explained that the electronic state of the thin films can be calibrated by electron-electron or electron-impurity scattering as the thin films have a high carrier concentration (~10^{20} cm^{-3}), namely, the many-body effect such as Coulomb interaction or exchange interaction which makes the band gap values decrease [14]. Obviously, such a scattering phenomenon is slight in the AZO thin films developed in this study.

Figure 6 shows the resistivity of the H_2-deposited and plasma-treated 2% H_2-deposited AZO thin films. The higher conductivity of transparent conduction oxide (TCO) thin films results mainly from deviations in stoichiometric compositions due to dopants or substitution atoms. The resistivity of transparent conduction oxide (TCO) thin films is proportional to the reciprocal of the product of carrier concentration N and mobility μ as follows:

$$\rho = \frac{1}{Ne\mu}. \tag{5}$$

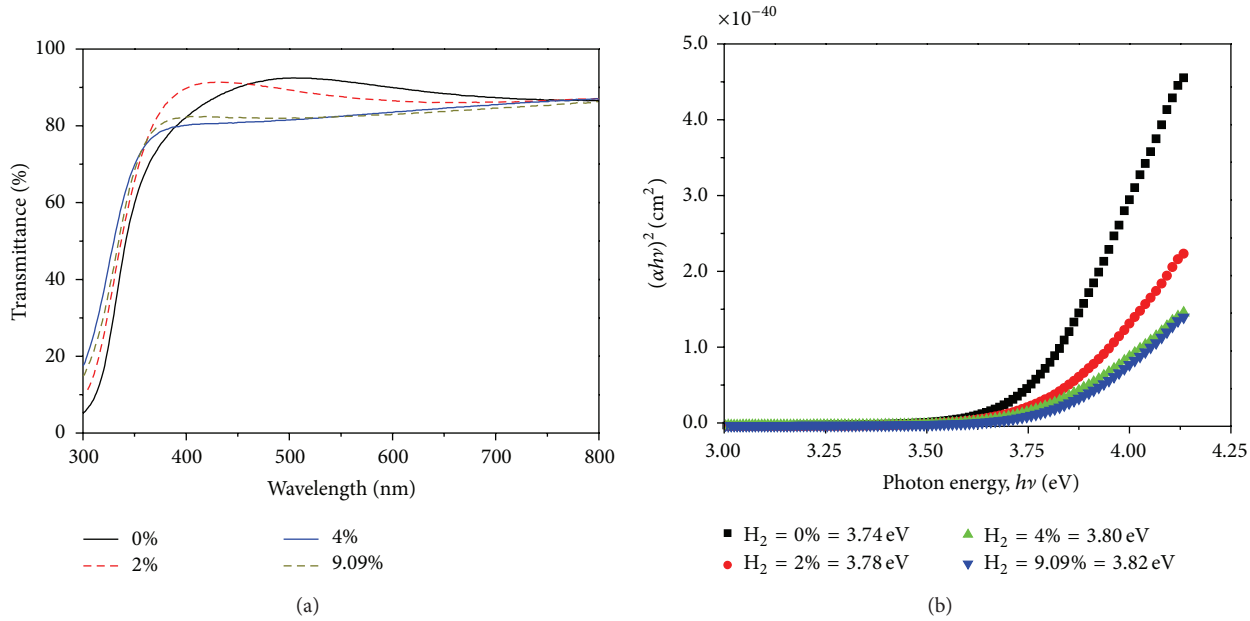

FIGURE 3: (a) Transmittance and (b) $(\alpha h\nu)^2$ versus $h\nu$-E_g plots of the H_2-deposited AZO thin films as a function of H_2 flowing rate.

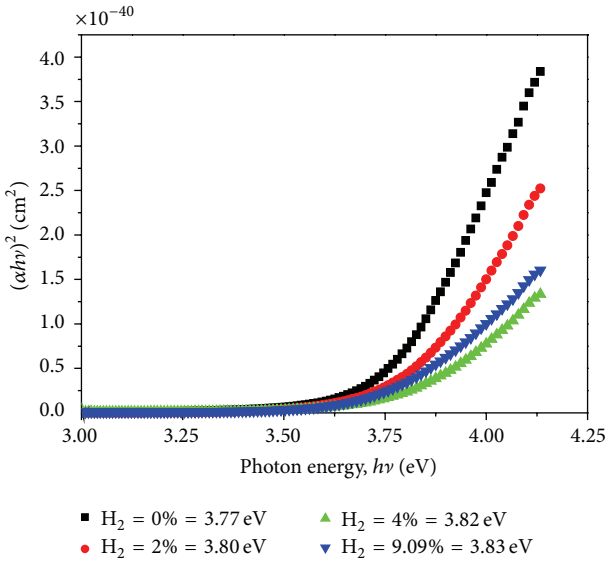

FIGURE 4: $(\alpha h\nu)^2$ versus $h\nu$-E_g plots of the plasma-treated AZO thin films as a function of H_2 flowing rate.

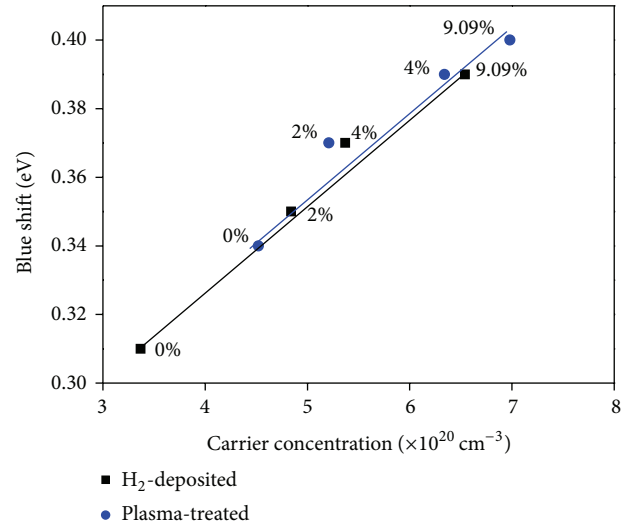

FIGURE 5: Blue-shift of the H_2-deposited and the plasma-treated AZO thin films as a function of H_2 flowing rate.

Electrons generated from oxygen vacancies and Zn interstitial atoms resulting from the dopant primarily determine the conduction properties of TCO thin films. Therefore, the electrical conductivity of AZO thin films will have large variations due to introducing H_2 in Ar during the sputtering deposition process.

The resistivity of AZO thin films deposited in pure Ar ambient was $25.2 \times 10^{-4}\,\Omega$-cm. However, the resistivity of the 2% H_2-deposited AZO thin films was $13.72 \times 10^{-4}\,\Omega$-cm deposition atmosphere, and the minimum resistivity of $12.67 \times 10^{-4}\,\Omega$-cm existed in the plasma-treated 2% H_2-deposited AZO thin films. As the H_2 rate was increased to 4%, the resistivity of the H_2-deposited AZO under H_2 + Ar atmosphere was beyond that of Ar-deposit ones. When AZO thin films are deposited on a glass substrate, many defects result and inhibit electron movement. In addition, too many oxygen vacancies may lead to an increase in scattering centers and a resultant decrease in mobility. The resistivity of AZO thin films decreases with the effects of hydrogen flow rate and hydrogen plasma, probably because the number of defects declines as the crystallization improves with H^+ ions for the crystal structure which boosts the deposition atoms' mobility.

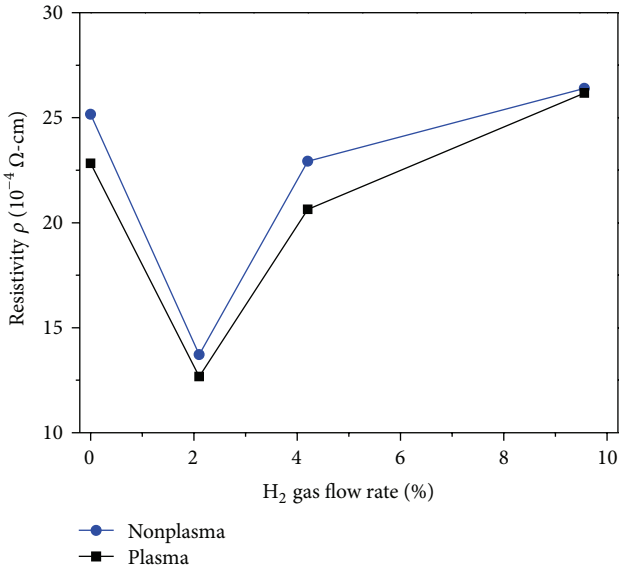

Figure 6: Resistivity (ρ) of the as-deposited and the plasma-treated AZO thin films as a function of H_2 flowing rate.

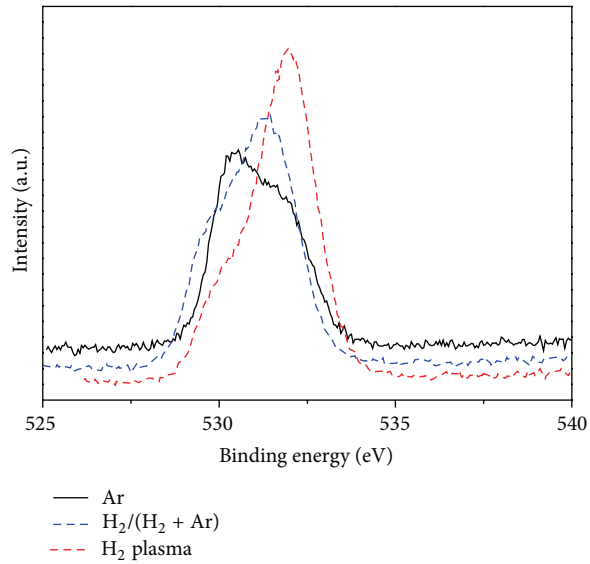

Figure 7: XPS spectra and their Gaussian-resolved components of O 1 s of the as-deposited and the plasma-treated AZO thin films as a function of H_2 flowing rate.

There are two kinds of donors contributing in AZO thin films' conductive mechanism. One is the native donor including interstitial Zn or oxygen vacancy and the other is substitutional Al atom. As 2% H_2 flow rate is used, a strong influence on oxygen extracts it from AZO thin films, which results in more vacancies to enhance the carrier concentration, and the conductivity has been improved. There are some scattering mechanisms occurring in AZO thin films which mainly include the neutral and ionized impurities and the grain boundaries scattering. When H_2 flow rate is more than 2%, H_2 creates more oxygen vacancies and generates more defects and free carriers, both of the neutral and ionized impurities scattering centers should increase. Besides, a small quantity of hydrogen atoms situates in the Zn–O bond center to relax the surrounding atoms. For that, as the H_2 flow rate is more than 2%, the resistivity increases with increasing H_2 flow rate. In this study, 2% is the optimal H_2 content, because AZO thin films have the minimum resistivity.

To clarify the mechanism of improvement in resistivity, the chemical structures of the Ar-deposited, H_2-deposited, and plasma-treated AZO thin films were investigated by XPS. Figure 7 shows the XPS spectra for their Gaussian-resolved components of O 1 s. As shown in Figure 7, a shoulder was visible on the high-energy side of the Ar-doped AZO thin films, indicating that at least two different bonds exist. The bonding state of O 1s spectrum of the Ar-doped AZO thin films is resolved into two components centered at 530.55 eV and 532.55 eV, respectively. The low bonding energy component centered at 530.55 eV is attributed to O^{2-} ions on the wurtzite structure of the hexagonal Zn^{2+} ion array, surrounded by Zn atoms with their full complement of nearest neighbor O^{2-} ions [15]. The high bonding energy component centered at 532.55 eV is attributed to the existence of adsorbed O_2 on the surfaces of the AZO thin films [16, 17]. For the 2% H_2-deposited AZO thin films, the O 1s peak slightly shifted to the high energy side and was located at 531.95 eV. After plasma treatment, the O 1 s peak of the 2% H_2-deposited AZO thin films shifted to the low energy side and was located at 531.25 eV. Unfortunately, these contributions from the surface cannot be separated from the main signal and might differ between samples. Binding energies from 531 eV to 532 eV are found for hydroxides and bonding energies from 530 eV to 530.8 eV are found for oxides. However, a Gauss-Lorentz fits of the 2% H_2-deposited and plasma-treated AZO thin films yield the main peaks at 531.25 eV and 531.95 eV for $Zn(OH)_2$. Our attributions are feasible and lie in the range of values found in other literature. From the XPS measurements, it can be concluded that the $Zn(OH)_2$ is found in the 2% H_2-deposited and plasma-treated AZO thin films, because the H_2 is existed from the surface into the crystal [18].

4. Conclusions

The effects of different hydrogen ($H_2/(H_2 + Ar)$, 0%~9.09%) flow rates (deposition temperature was 200°C) added during the deposition process of AZO thin films were investigated. The Burstein-Moss shift effects were measured and used to prove that the defects in AZO thin films decreased with increasing H_2 flow rate. The value variations in the optical band gap (E_g) of the H_2-deposited and plasma-treated AZO thin films were evaluated from the plots of $(\alpha h\nu)^2 = c(h\nu - E_g)$, and the E_g values increased with increasing hydrogen flow rate. As the hydrogen flow rate increased from 0 to 9.09%, the calculated E_g values increased from 3.74 eV to 3.82 eV, and the E_g values of the plasma-treated AZO thin films increased from 3.77 eV to 3.83 eV. From the XPS measurements, it could be concluded that $Zn(OH)_2$ was formed in the H_2-deposited and plasma-treated AZO thin films. The resistivity of AZO thin films decreased with

increasing hydrogen flow rate and reached a minimum value of 13.56×10^{-4} Ωcm at a H_2 flow rate of 2%, the minimum resistivity of 12.67×10^{-4} Ω-cm existed in the plasma-treated 2% H_2-deposited AZO thin films.

Conflict of Interests

The authors declare that there is no conflict of interests regarding the publication of this paper.

Acknowledgments

The authors acknowledge the financial support of NSC 101-2221-E-005-065, NSC 102-2622-E-390-002-CC3, and NSC 102-2221-E-390-027.

References

[1] S. Major, S. Kumar, M. Bhatnagar, and K. L. Chopra, "Effect of hydrogen plasma treatment on transparent conducting oxides," *Applied Physics Letters*, vol. 49, no. 7, pp. 394–396, 1986.

[2] L. Stolt, J. Hedström, J. Kessler, M. Ruckh, K. Velthaus, and H. Schock, "ZnO/CdS/$CuInSe_2$ thin-film solar cells with improved performance," *Applied Physics Letters*, vol. 62, no. 6, pp. 597–599, 1993.

[3] D. H. Zhang and D. E. Brodie, "Effects of annealing ZnO films prepared by ion-beam-assisted reactive deposition," *Thin Solid Films*, vol. 238, no. 1, pp. 95–100, 1994.

[4] J. Chevallier, B. Theys, A. Lusson, C. Grattepain, A. Deneuville, and E. Gheeraert, "Hydrogen-boron interactions in p-type diamond," *Physical Review B—Condensed Matter and Materials Physics*, vol. 58, no. 12, pp. 7966–7969, 1998.

[5] C. G. van de Walle, "Hydrogen in semiconductors and insulators," *Journal of Alloys and Compounds*, vol. 446-447, pp. 48–51, 2007.

[6] B. Y. Oh, M. C. Jeong, and J. M. Myoung, "Stabilization in electrical characteristics of hydrogen-annealed ZnO:Al films," *Applied Surface Science*, vol. 253, no. 17, pp. 7157–7161, 2007.

[7] Y. M. Strzhemechny, H. L. Mosbacker, D. C. Look et al., "Remote hydrogen plasma doping of single crystal ZnO," *Applied Physics Letters*, vol. 84, no. 14, pp. 2545–2547, 2004.

[8] F. H. Wang, H. P. Chang, C. C. Tseng, and C. C. Huang, "Effects of H_2 plasma treatment on properties of ZnO:Al thin films prepared by RF magnetron sputtering," *Surface and Coatings Technology*, vol. 205, no. 23-24, pp. 5269–5277, 2011.

[9] T. S. Moss, "The interpretation of the properties of indium antimonide," *Proceedings of the Physical Society B*, vol. 67, no. 10, pp. 775–782, 1954.

[10] E. Burstein, "Anomalous optical absorption limit in InSb," *Physical Review*, vol. 93, no. 3, pp. 632–633, 1954.

[11] I. Hamberg, C. G. Granqvist, K. F. Berggren, B. E. Sernelius, and L. Engström, "Band-gap widening in heavily Sn-doped In_2O_3," *Physical Review B—Condensed Matter and Materials Physics*, vol. 30, no. 6, pp. 3240–3249, 1984.

[12] N. Serpone, D. Lawless, and R. Khairutdinov, "Size effects on the photophysical properties of colloidal anatase TiO_2 particles: size quantization or direct transitions in this indirect semiconductor?" *The Journal of Physical Chemistry*, vol. 99, no. 45, pp. 16646–16654, 1995.

[13] B. Y. Oh, M. C. Jeong, W. Lee, and J. M. Myoung, "Properties of transparent conductive ZnO:Al films prepared by co-sputtering," *Journal of Crystal Growth*, vol. 274, no. 3-4, pp. 453–457, 2005.

[14] K. H. Kim, K. C. Park, and D. Y. Ma, "Structural, electrical and optical properties of aluminum doped zinc oxide films prepared by radio frequency magnetron sputtering," *Journal of Applied Physics*, vol. 81, no. 12, pp. 7764–7772, 1997.

[15] B. H. Choi, H. B. Im, J. S. Song, and K. H. Yoon, "Optical and electrical properties of Ga_2O_3-doped ZnO films prepared by r.f. sputtering," *Thin Solid Films*, vol. 193-194, part 2, pp. 712–720, 1990.

[16] M. Chen, X. Wang, Y. H. Yu et al., "X-ray photoelectron spectroscopy and auger electron spectroscopy studies of Al-doped ZnO films," *Applied Surface Science*, vol. 158, no. 1, pp. 134–140, 2000.

[17] H. Sato, T. Minami, S. Takata, T. Mouri, and N. Ogawa, "Highly conductive and transparent ZnO:Al thin films prepared on high-temperature substrates by d.c. magnetron sputtering," *Thin Solid Films*, vol. 220, no. 1-2, pp. 327–332, 1992.

[18] W. Eisele, A. Ennaoui, P. Schubert-Bischoff et al., "XPS, TEM and NRA investigations of Zn(Se,OH)/$Zn(OH)_2$ films on Cu(In,Ga)$(S,Se)_2$ substrates for highly efficient solar cells," *Solar Energy Materials and Solar Cells*, vol. 75, no. 1-2, pp. 17–26, 2003.